Conformational Changes of Linear−Dendrimer Diblock Copolymers in Dilute Solution

Leslie M. Passeno,[†,‡] Michael E. Mackay,*[,†] and Gregory L. Baker[‡]

Department of Chemical Engineering and Materials Science and Department of Chemistry, Michigan State University, East Lansing, Michigan 48823

Robert Vestberg and Craig J. Hawker

Materials Research Laboratory, University of California, Santa Barbara, California 93106

Received August 3, 2005; Revised Manuscript Received November 5, 2005

ABSTRACT: The conformation of linear−dendrimer hybrid diblock copolymers in solution has been studied using both small-angle neutron scattering and dynamic light scattering. The diblock consisted of a fourth-generation benzyl ether dendrimer with different molecular weight polystyrene bonded to the focal point of the dendrimer; the total molecular weight ranged from 20 to 100 kDa. In agreement with previous studies, it was found that this dendron, without a linear chain attached, alters its size upon solvent change. The addition of a polystyrene chain to the focal point of a dendrimer was also found to have an effect on the dimensions and shape of the dendrimer block. A low-molecular-weight polystyrene chain swelled the dendrimer without perturbing its native spherelike conformation. However, at larger polystyrene molecular weights, the linear block manipulates a transition of the dendrimers' morphology form spherelike to an extended conformation. Control of this shape and size change has potential for these unique macromolecular architectures to function as a novel molecular building block.

Introduction

Dendrimers or dendrons are a unique class of macromolecules that have a specific molecular weight, large number of terminal groups, and well-defined architecture consisting of branched units emanating from a focal point.[1−3] These unique characteristics have triggered numerous studies to use dendrimers in applications such as drug delivery,[4] light harvesting,[5] and reaction catalysis.[6] It is clear that the dendrimer molecular architecture dictates its physical properties and thus enables such diverse applications to be explored. In addition, synthetic modification of dendrimers at both the focal point[7,8] and the end groups[9−11] has proven successful in expanding their utility. Further, block copolymers consisting of a linear polymer attached to the focal point[12−21] have promising applications due to their architectural asymmetry.[12−15]

To take full advantage of linear−dendrimer diblock copolymers' properties, the conformation in both solution and the bulk must be understood. In prior studies, the phase behavior of these molecules in the bulk has been proven to be different from traditional linear−linear diblock copolymers due to the architectural differences between each block.[12−21] It was found that both the generation number and the molecular weight of the linear chain dictated which morphology the hybrid diblock copolymer adopted.

The solution behavior of these diblocks has also been shown to be unique and significantly affected by the molecular asymmetry between the two blocks. For example, Gistov and Fréchet[22] have investigated the solution properties of poly(benzyl ether) (PBE)−poly(ethylene oxide) (PEO) diblocks which are dominated by this molecular asymmetry. Since the dendrimer and linear blocks have different solubility parameters, they examined how the solvent quality affected the intrinsic viscosity and solubility of the system as compared to linear PEO analogues. The solution behavior of generation 4 (G4) PBE dendrimer−PEO chain was reported to be a function of the PEO molecular weight, and with PEO molecular weights of 26 and 46 kDa the intrinsic viscosity values were lower than that of pure PEO when in THF. This is a marginal solvent for PEO and a good solvent for the dendrimer, thus indicating the entire molecule was in a collapsed state compared to the linear chain. When the system was placed in a methanol/water solution, which is a good solvent for the linear block and a poor solvent for the dendrimer block, the solubility of the diblocks was dependent on the molecular weight of the linear chain being large enough to allow unimolecular micelle formation. These results indicate that the hybrids' conformations are a function of both the chain molecular weight and dendrimer generation.

A hybrid system containing a PBE dendron block was studied via intrinsic viscosity by Jeong et al.[23] Here, a G4-PBE dendrimer with a linear poly(styrene) (PS) chain attached to its focal point was investigated and showed interesting behavior with an increase of the PS chain molecular weight. In particular, when compared to the intrinsic viscosity of linear PS, the smaller molecular weight hybrids had an intrinsic viscosity lower than a PS chain of equal molecular weight. However, a sudden intrinsic viscosity increase was observed for the hybrids between molecular weights of 60 and 80 kDa and was equal to that of linear PS for molecular weights greater than 80 kDa. This suggests the overall molecular conformation of the hybrid changes with respect to the relative molecular weight of the two blocks.

While the intrinsic viscosity studies hint there is a conformational transformation capability of the PBE−PS hybrids, it is difficult to infer whether one or both of the blocks change conformation. All studies of linear−dendrimer diblock copolymers in solution thus far have focused on the conformation of the entire system.[17,22,23] A full understanding of the system necessitates pinpointing the relative locations and morphology

* Corresponding author: e-mail mackay@msu.edu.
[†] Department of Chemical Engineering and Materials Science.
[‡] Department of Chemistry.

10.1021/ma0517291 CCC: $33.50
Published on Web 12/21/2005

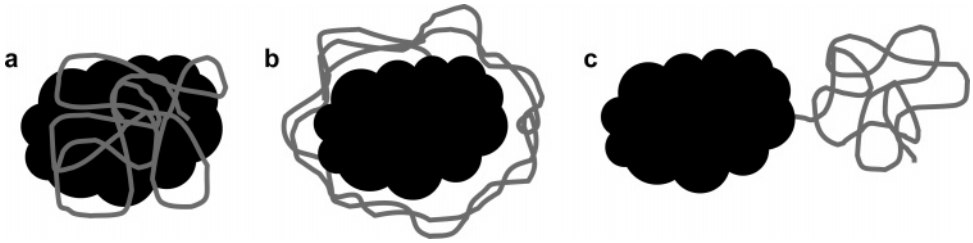

Figure 1. Three potential conformational states of linear−dendrimer diblocks in solution: (a) knitted coil, (b) encapsulated dendrimer, and (c) random coil.

Table 1. Sample Codes and Number-Average Molecular Mass (*M*) of Compounds Used in This Study[a]

sample code	*M*-dendrimer (Da)/ *M*-polystyrene (kDa)/*M* (kDa)	PDI[b]	sample code	*M*-dendrimer(Da)/ *M*-polystyrene (kDa)/*M* (kDa)	PDI[b]
G4	3288/0/3288	~1	dPS-156K	0/156/156	1.19
G4-dPS-20K	3288/16.7/20	1.06	G4-PS-46K	3288/42.7/46	1.09
G4-dPS-45K	3288/41.7/45	1.08	G4-PS-70K	3288/66.7/46	1.11
G4-dPS-100K	3288/96.7/100	1.12	G4-PS-91K	3288/87.7/91	1.15
dPS-21K	0/21/21	1.04	PS-44K	0/44.1/44.1	1.07
dPS-63.5K	0/63.5/63.5	1.10	PS-75K	0/75.2/75.2	1.17
dPS-83K	0/83/83	1.16	PS-115	0/115.3/115.3	1.08

[a] *M*-dendrimer represents the mass of the dendrimer, *M*-polystyrene the mass of the polystyrene, and *M* the total mass. [b] The polydispersity index, PDI, is defined as the weight- to number-average molecular mass ratio.

of each block. Figure 1 illustrates three possible linear−dendrimer diblock conformational states in solution for a system where the linear and dendrimer blocks are compatible with each other. Each conformational state pertains to different relative locations of the two blocks.[24] The first state is a knitted coil, where the linear chain weaves in and out of the dendrimer; thus, the dendrimer shields or partially shields the linear polymer from the surrounding environment. For this to occur, the dendrimer must have enough free volume to accommodate the linear block. A second hybrid conformation consists of the linear chain wrapping itself around the dendrimer, thus shielding the dendrimer from the surroundings and forming a unimolecular micelle. This encapsulated dendrimer state would occur when the linear block is compatible with the surrounding medium and the dendrimer less compatible, resulting in a core−shell morphology. A third potential molecular arrangement consists of the linear chain completely expelled from the cavities within the dendrimer. This could occur if there is not enough free volume within the dendrimer to contain the entire linear chain and each component has similar solubility in the solvent.[23]

Distinguishing between these three states requires knowledge of the relative block locations, which will be performed for the G4-PBE−PS hybrid in the present work. We studied three different molecular weight hybrids: 20, 45, and 100 kDa, which is the sum of the G4-PBE dendrimer (M = 3288 g/mol) and linear chain molecular weights, and thus the only difference between the three hybrids is the molecular weight of the linear block. The PS chain was also deuterated (dPS) to allow small-angle neutron scattering (SANS) to individually visualize each block though a series of contrast matching experiments.[25] This information can be used to ascertain the architectural structure of the two blocks.

Experimental Section

Materials. Poly(benzyl ether) dendrimers were prepared according to a previous procedure.[2] The third generation (G3) bromides were coupled with a 3,5-dihydroxylbenzyl-functionalized alkoxyamine initiator.[26] The purified fourth-generation (G4) dendritic initiators were then used to prepare the hybrid dendrimer−linear diblock copolymers by standard living free radical conditions. The linear polystyrene block degree of polymerization is controlled by the molar ratio of dendritic initiator to monomer. Deuterated solvents were purchased from Aldrich Chemical Co. (St. Louis, MO) and used as received.

SANS. Measurements were taken at the small-angle neutron diffractometer (SAND) at Argonne's Intense Pulsed Neutron Source. A sample-to-area detector distance of 2.0 m was used. The radiation had a wavelength range of 1−14 Å, making the total wave vector (Q) range covered 0.0034−0.6 Å^{-1}, where $Q = 4\pi \sin(\theta/2)/\lambda$ with θ and λ defined as the scattering angle and radiation wavelength, respectively. Measurements were taken at room temperature. Low concentrations were used for each sample to generate sufficient scattering in the allotted time while minimizing intermolecular scattering effects.[25] Hence, consistent power laws were not observed for plots of radius vs molecular mass due to concentration effects, particularly for the higher molecular weight samples. Note the effect of concentration on the size of polymers has been extensively studied before;[27−29] here the radius of differing morphologies were compared at a particular (low) concentration. Samples were filtered through a 0.1 μm Whatman Anodisc 13 filter and sonicated for 20 min and placed in a hermetically sealed quartz cell for the scattering experiments. A list of samples is given in Table 1.

When the scattering length density (SLD) of the solvent matches that of the scatterer, there is a contrast match, and no coherent scattering occurs. Deuterating the linear chain makes the two blocks' SLD quite different, with the dendrimer block having a SLD of 2.03×10^{-6} Å^{-2} and the dPS a SLD of 6.42×10^{-6} Å^{-2}. When the G4-dPS hybrid is placed in d_8-THF (SLD = 6.35×10^{-6} Å^{-2}), the dPS chain is essentially contrast matched with the solvent and scattering only occurs from the dendrimer block. The linear block was investigated using a solvent combination of 79:21 h_6-benzene: d_6-benzene (SLD of 2.07×10^{-6} Å^{-2}) which provides a contrast match to the G4-PBE dendrimer, and thus scattering only occurs from the linear block. Performing both of these contrast match experiments on the three molecular weight hybrids and comparing the behavior of each block to that of a native PBE dendrimer or dPS chain in the same solvent allowed the conformation of each block to be determined as well as the overall conformation of the diblock.

Neutron scattering data for hybrids were analyzed in the Guinier regime.[30] This analysis allowed for quick determination of the shape and size of the dendrimer as models for compact objects, rods, and sheets were applied to all samples. The scattering intensity, $I(Q)$, in the low-Q regime was evaluated using the expression for compact ("spherelike") objects with a given radius of gyration (R_g)[31]

$$I(Q) \approx \phi V(\Delta\rho)^2 \exp\left(-\frac{Q^2R_g^2}{3}\right) \equiv I(0) \exp\left(-\frac{Q^2R_g^2}{3}\right) \quad (1)$$

where ϕ is volume fraction of scattering centers, V the volume of each scattering center, $(\Delta\rho)^2$ the square of the difference of the solvent and the scatterer SLD, and $I(0)$ the intensity at zero wave vector. The slope resulting from a plot of $\ln(I(Q))$ vs Q^2 in the region where $QR_g \cong 1$ allows R_g to be obtained. The radius of a homogeneous, constant-density sphere is determined from the R_g by $R_g = 0.775R$.

A modified Guinier analysis for rodlike objects approximates the scattering intensity in the low-Q regime by[31]

$$QI(Q) \approx \frac{\pi\phi V(\Delta\rho)^2}{L} \exp\left(\frac{-Q^2R_c^2}{2}\right) \equiv QI(0) \exp\left(\frac{-Q^2R_c^2}{2}\right) \quad (2)$$

Here, L is the rod length and R_c is the root-mean-square of the distances of all of the atoms in a cross section of the rod to the centroid of this cross section determined from the slope in a plot of $\ln(Q(I(Q))$ vs Q^2, in the region of Q where $QR_c \cong 1$. The radius of the rod (R_r) is obtained by $R_c\sqrt{2}$. A sheetlike particle, which is much smaller in one dimension than the other two, has[31]

$$Q^2I(Q) \approx \frac{2\pi\phi V(\Delta\rho)^2}{A} \exp\left(\frac{-Q^2T^2}{12}\right) \equiv Q^2I(0) \exp\left(\frac{-Q^2T^2}{12}\right) \quad (3)$$

where A is the area of the particle and T the sheet thickness and is valid when $QT < \sqrt{12}$.

To determine the goodness of each Guinier fit, the experimental value of $I(0)$ or $QI(0)$ was used to determine the amount of solvent within each sample and check that the mass density of the swollen dendrimer is reasonable. The numerical prefactors of eqs 1 and 2 were set equal to the experimental value of $I(0)$ and $QI(0)$, respectively, and then solved for $(\Delta\rho)^2$. Using this value of $(\Delta\rho)^2$ and the scattering length density of the solvent (ρ_{solv}), we calculated the scattering length density of the scatterers (ρ_{scat}), which includes solvent and dendrimer. We calculated the amount of solvent within the dendrimer by

$$\rho_{scat} = [\rho_{solv}]\theta + [1 - \theta]\rho_{sample} \quad (4)$$

where θ is the mass fraction of solvent within the scatterer and ρ_{sample} is the scattering length density of the dendrimer.

Neutron scattering data were also analyzed by fitting I vs Q to the form factor of a solid sphere or Gaussian coil when appropriate. We also used Holtzer plots[32] to reveal coillike and rodlike behavior. These graphs are included in the Supporting Information.

Dynamic Light Scattering (DLS). Measurements were performed with a Protein Solutions Dyna Pro-MS/X system with temperature control. All samples were filtered as described above and allowed to equilibrate in the instrument for 25 min at 25 °C before measurements were taken, resulting in calculation of the hydrodynamic radius (R_h). The sample is illuminated by a semiconductor laser with ~830 nm wavelength. The light scattered at an angle of 90° is collected and guided via a fiber-optic cable to an actively quenched, solid-state single photon counting module (SPCM), where the photons are converted to electrical pulses and correlated. Autocorrelation is used to analyze the time scale of the scattered light intensity fluctuations. The uniformity of the sample sizes is determined by a monomodal curve fit, cumulants, which assumes a single particle size with a Gaussian distribution.

Results and Discussion

The molecular morphology of the G4-PBE dendron samples was investigated in both d_6-benzene and d_8-THF using the three Guinier analyses mentioned above to determine the influence of solvent on the size and shape of the dendrimer block. The dendrimers behave as spherelike objects in both d_6-benzene and d_8-THF due to the observed negatively sloped straight line in the Guinier plots for compact objects (Figure 2). It is evident from the Guinier fits in Figure 2 that the dendrimer is larger in d_6-benzene than in d_8-THF, with radii values of 1.73 ± 0.03 and 1.35 ± 0.04 nm, respectively. These sizes agree reasonably well with radii values reported by Tande et al.[12] of 1.93 ± 0.1 and 1.50 ± 0.1 nm in d_6-benzene and d_8-THF, respectively. Using the experimental value of $I(0)$ (Table 2), the mass fraction of solvent (θ) within the dendrimer was calculated by eq 4 as described above and found to be 0.45 and 0.51 for d_8-THF and d_6-benzene, respectively.

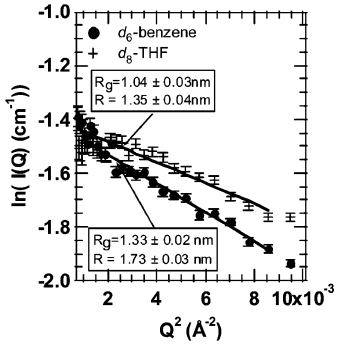

Figure 2. Guinier analysis for G4-PBE dendrons in d_6-benzene and d_8-THF at a concentration of 50 mg/mL; data fit for a compact (spherelike) object.

The G4-PBE dendrimer is larger than the minimum radius it can have in solution which is 1.09 nm when in chloroform, close to the value expected if the dendrimer collapses to its bulk density,[23] indicating the dendrimer is in an expanded state in both d_6-benzene and d_8-THF. A solvent dependence on size is a well-known property of linear polymers and has been previously observed in dendrimers.[23] While the dendrimer size has changed with solvent type, the shape has remained "spherelike". Further contrast variation studies of the dendrons need be conducted to determine the overall segment distribution and whether this distribution changes with solvent.[33−35]

These structural changes may be delineated in part by measuring the hydrodynamic radius, R_h, of the G4-PBE dendrimers in both d_6-benzene and d_8-THF. An R_h of 1.70 ± 0.02 nm was obtained in both solvents, making the ratio of $R_g/R_h = 0.79 \pm 0.03$ for d_8-THF solvent and 1.02 ± 0.03 for d_6-benzene. This ratio is a quantitative indicator of molecular conformation,[36] where an R_g/R_h ratio of $\sqrt{(3/5)} \approx 0.775$ is indicative of a constant density, homogeneous sphere. A value of 1.50 is descriptive of a monodisperse Gaussian coil in a Θ solvent, and a value of 1.78 represents linear polymers in a good solvent[36,37] although experiments show values of 1.16 and 1.27 for linear polymers in Θ solvents.[38,39] The R_g/R_h ratios for the dendrimer illustrate a more spherelike nature in both d_8-THF and d_6-benzene, indicating a significantly different structure in solution as compared to random-coil linear polymers under analogous conditions. The ratio also suggests the dendron behaves as a constant density (expanded) sphere in d_8-THF, implying backfolding of end groups.[40,41] It should be noted that this effect is not due to poor dendrimer−solvent interactions as the solubility parameter of the dendrimer has been found to be similar to that of benzene and THF while the radius of the dendrimer is larger in both solvents than the minimum possible value of 1.09 nm.[23]

The dendrimer block conformation within the hybrid block copolymers was determined by dissolving the G4-PBE−dPS diblocks in d_8-THF, which is a contrast match for the dPS block. Two different concentrations were analyzed, 4 and 50 mg/mL, for the hybrids with molecular weights of 20, 45, and 100 kDa,

Table 2. Values for R_g and R_c Determined from Guinier Analyses Described in the Text at a Concentration of 50 mg/mL[a]

sample code	G4	G4	G4-dPS-20K	G4-dPS-45K	G4-dPS-100K
solvent	d_8-THF	d_6-benzene	d_8-THF	d_8-THF	d_8-THF
scattering from	dendrimer	dendrimer	dendrimer	dendrimer	dendrimer
R_g (nm)[a]	1.04 ± 0.03	1.33 ± 0.02	1.40 ± 0.01	na[b]	na
$I(0)_{exp}$[c] (cm^{-1})	0.241 ± 0.002	0.245 ± 0.002	0.062 ± 0.003	na	na
$Q_{max}R_g$	0.919	1.13	1.35	na	na
R_c (nm)[d]	na[e]	na	na	2.70 ± 0.28	2.62 ± 0.29
$QI(0)_{exp}$[f] ($Å^{-1}\,cm^{-1}$)	na	na	na	$(2.50 \pm 0.4) \times 10^{-3}$	$(3.7 \pm 2.0) \times 10^{-3}$
$Q_{max}R_c$	na	na	na	1.006	0.976
θ[g]	0.45	0.51	0.56	0.82	0.78

[a] Symbols are explained in the text while Q_{max} is the maximum Q value used in the regression. [a] Radius of gyration for a spherelike object. [b] Attempts to fit data to a spherelike object failed for these samples. [c] Experimental value of $I(0)$ from a spherelike object Gunier plot (eq 1). [d] Cross-sectional radius for a rod. [e] Attempts to fit data to a rodlike object failed for these samples. [f] Experimental value of $QI(0)$ from a rodlike object Gunier fit (eq 2). [g] θ is the mass fraction of solvent within the scatterers.

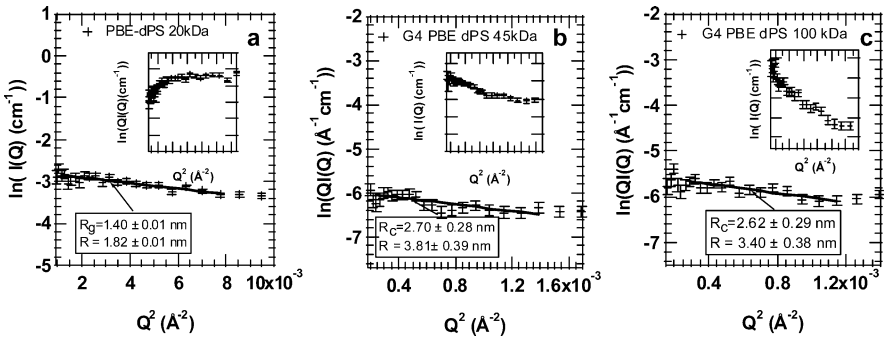

Figure 3. (a) Guinier analysis for PBE−dPS 20 kDa system in d_8-THF at a concentration of 50 mg/mL; dendrimer block is scattering as a spherelike object. Inset is a modified Guinier analysis for a rodlike object, which does not represent the data. (b) Rodlike Guinier analysis for PBE−dPS 45 kDa hybrid in d_8-THF at a concentration of 50 mg/mL. Inset shows the attempted representation of data to Guinier fit for compact object. (c) Rodlike Guinier analysis for PBE−dPS 100 kDa hybrid in d_8-THF at 50 mg/mL. Inset is the Guinier analysis for compact object, which is a poor fit due to curvature

noting there are insignificant differences observed for the dendrimer block size at these two concentrations.

By fitting the scattering data of the G4-PBE−dPS 20 kDa hybrid in d_8-THF at a concentration of 50 mg/mL with a Guinier analysis for compact objects (eq 1), Figure 3a, a radius for the dendrimer block of 1.82 ± 0.01 nm was found, which is appreciably larger that the radius of the "free" dendrimer in the same solvent, 1.35 ± 0.04 nm. The mass fraction of solvent and dPS within the dendrimer is 0.56 (Table 2), which is higher than the value for the corresponding free dendrimer in d_8-THF, 0.45. Since the hybrids' dendrimer block is more swollen than the corresponding free dendrimer, this means there is more mass, i.e., linear dPS block and solvent, occupying the free volume within the dendrimer. Attempts made to fit scattering data for the dendron as a rodlike object (eq 2) failed as shown in the inset of Figure 3a. The sheetlike architecture (eq 3) was similarly found to not represent the scattering data for any of the samples and will not be mentioned further.

The dendrimer block of the next higher molecular weight G4-PBE−dPS hybrid (45 kDa) was subsequently studied in d_8-THF at a concentration of 50 mg/mL using a Guinier analysis for compact objects (see Figure 3b). Attempts to make a linear fit with the "spherelike" morphology failed, as displayed in the inset of Figure 3b evidenced by nonlinear behavior at small Q. The Guinier analysis for rodlike objects (eq 2) proved successful (Figure 3b) with a substantial increase in the dendron size with an R_c value of 3.81 ± 0.39 nm, which is comparable to the maximum possible radius of ~3.6 nm the dendrons' bonds can adopt in an a fully extended state. This is a much larger dendrimer radius as compared to both the "free" dendrimer radius, 1.35 ± 0.04 nm, and the dendrimer block of the 20 kDa hybrid, 1.82 ± 0.01 nm, and will be discussed in greater detail below.

We performed a Guinier analysis for the G4-PBE−dPS 100 kDa hybrid in d_8-THF at a concentration of 50 mg/mL and found that the dendrimer block behaves analogously to that of the 45 kDa system, scattering as a rodlike object as opposed to a sphere (Figure 3c). The model fit results in a dendrimer radius of 3.40 ± 0.38 nm, which matches the size of the 45 kDa dendrimer block considering experimental error. As for the 45 kDa system, attempts to fit the 100 kDa hybrid's data to a Guinier analysis for a sphere failed due to nonlinear behavior at small values of Q (inset of Figure 3c).

These contrast match experiments have revealed that the dendrimer block's size and shape is dependent upon the linear block molecular weight. The G4-PBE−dPS 20 kDa hybrid has a dendrimer block where the branches adopt a "spherelike" shape (Figure 3a), just as the free dendrimer in solution (Figure 2), yet the size of this sphere is ~35% larger in the hybrid system (>2× change in volume). The difference in size between the hybrid's dendrimer block and the free dendrimer in solution is probably due to the linear chain occupying space within the dendrimer, resulting in swelling and possible development of the knitted coil morphology shown in Figure 1.

The two higher molecular weight systems, G4-PBE−dPS 45 kDa (Figure 3b) and G4-PBE−dPS 100 kDa (Figure 3c) did not show the expanded spherelike morphology, and instead these two systems have dendrimer blocks that are "rodlike" in shape (eq 2). According to the model, the cylinder radius for the 45 and 100 kDa systems has values of 3.81 ± 0.39 and 3.40 ± 0.38 nm, respectively, making the cylinder length of order 0.1 nm, suggesting a disklike morphology. Fitting the I vs Q data with the disk form factor, similar in form to eq 3, was unsuccessful.

Further, because of the large solvent mass fractions of 0.82 and 0.78 calculated from the rodlike Guinier fit of the dendron

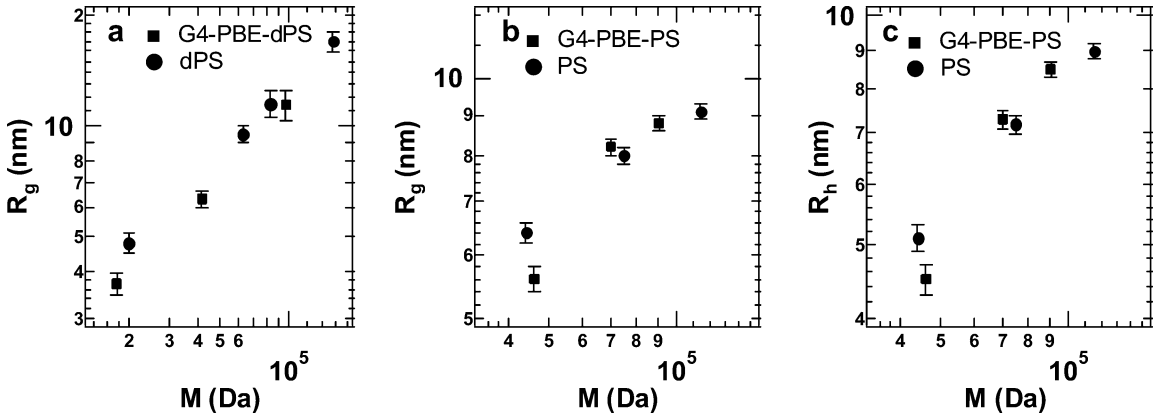

Figure 4. (a) A plot of radius of gyration vs molecular weight for both the dPS block of the hybrids and dPS in 79:21 h_6:d_6-benzene at 4 mg/mL. The two lower molecular weight hybrids fall below the size of the corresponding dPS linear chains, indicating a collapsed state for these two hybrids' linear block. (b) A plot of radius of gyration vs molecular weight for G4-PBE−PS hybrids and PS in d_8-THF at a concentration of 4 mg/mL. The 46 kDa G4-PBE−PS hybrid's size is below that of the corresponding PS linear chain, indicating a collapsed state. The 70 and 91 kDa G4-PBE−PS hybrids' R_g's are approximately equal to the corresponding linear PS chain's, indicating a noncollapsed state of these systems. (c) A plot of hydrodynamic radius vs molecular weight for G4-PBE−PS hybrids and PS in THF at a concentration of 4 mg/mL. The 46 kDa G4-PBE−PS hybrid's size is below that of the corresponding PS linear chain, indicating a collapsed state. The 70 and 91 kDa G4-PBE−PS hybrids' R_h is larger than the corresponding linear PS chain.

Table 3. Experimental *QI*(0) Values Were Set Equal to the Numerical Prefactor of the Guinier Expression for a Finite Sized Cone, Eq 5, with Various *R* Values Representing the Radius of the Cone's Base

sample code	R (nm)[a]	$(\Delta\rho)^2$ (cm^{-4})[b]	θ[c]
G4-dPS-45K[d]	2	8.68×10^{13}	0.32
	2.5	5.56×10^{13}	0.45
	3	3.86×10^{13}	0.55
G4-dPS −100K[d]	2	1.28×10^{13}	0.17
	2.5	8.22×10^{13}	0.34
	3	5.71×10^{13}	0.45

[a] Radius of cone's base, various values tried. [b] Experimental value of the difference in scattering length density between the scatterer and the solvent found by equating experimental *QI*(0) values to numerical prefactor in eq 5. [c] Mass fraction of solvent and possibly linear dPS within dendrimer, eq 4.

blocks of the 45 and 100 kDa systems, respectively (see Table 2), it is not expected that the dendrimer molecule adopts a rodlike conformation. Rather, it is believed that the actual conformation of the dendrimer block for the 45 and 100 kDa hybrids is that of a distorted wedge or "ice-cream cone". This molecular arrangement explains why a Guinier analysis for sheetlike objects did not work, and morphological equivalence between the cone and rod is expected to follow eq 2. In fact, the results given by Hjelm[42] show the Guinier expression for a finite size cone should follow (see Hjelm's eq 19)

$$QI(Q) \approx 0.2\phi R^2(\Delta\rho)^2 \exp\left(\frac{-Q^2[R_c^2]}{2}\right) \qquad (5)$$

for $Q < 1/L$ and where R is the radius of the cone's base and $[R_c^2]$ represents a "weight" average radius. The numerical prefactor in eq 5 reduces the value of $QI(0)$ to numbers of order 10^{-3} Å^{-1} cm^{-1}, in agreement with the experimental values given in Table 2 for a true rod. To justify the cone-shaped dendrimer block, we set the experimental values of $QI(0)$ equal to the numerical prefactor of eq 5 by using known values of ϕ and estimated value of R to find $(\Delta\rho)^2$ and θ, listed in Table 3. The resulting θ values are more reasonable than those from the rodlike fit (Table 2), indicating the dendrimer block is more conelike. While the exact dendron shape is difficult to fully ascertain, the data support that the free dendrimer and 20 kDa hybrid's dendron block shape is quite different from that of the 45 and 100 kDa hybrid's dendrimer block.

It is apparent that the relative molecular weight of the linear and dendrimer blocks plays a key role in the subsequent morphology of the dendrimer block; yet, complete information on the location of the two blocks in solution cannot be made without characterizing the linear block of the hybrids. This was done by placing the G4-PBE−dPS hybrids in a solution of 79:21 h_6-benzene:d_6-benzene, which is a contrast match for the dendrimer. The concentration used for these experiments was 4 mg/mL, and the radius of gyration of the linear block was obtained by plotting $I(Q)$ vs Q and fitting the profile to the form factor of a Gaussian coil.[33] To compare the behavior of the linear block to that of "free" dPS in the same solvent, we did scattering experiments on dPS with molecular weights of 18, 63, 83, and 155 kDa under the same conditions with similar data interpretation. A plot of the radius of gyration vs molecular weight was used to compare the size difference between the linear block of the hybrids to that of a free dPS chain of comparable molecular weight. Figure 4a shows that the two lower molecular weight hybrids, 20 and 45 kDa, have a linear block that falls below the size of the analogous "free" dPS chain, indicating the dPS block of the hybrid is in a more compact state for these two systems. The 100 kDa hybrid's linear block is approximately the same size as the "free" linear chain, suggesting that it expands in solution to the size of the corresponding dPS chain. These results match the intrinsic viscosity data of Jeong et al.,[23] who studied the analogous nondeuterated forms of the hybrids in benzene.

To verify that the observations for the contrast match experiments are independent of solvent type and deuteration effects, we performed two additional series of experiments. First, the size of G4-PBE−PS hybrids with molecular weights of 46, 70, and 91 kDa in d_8-THF was compared to PS in d_8-THF; all solutions were at a concentration of 4 mg/mL (see Figure 4b). The radius of gyration for the G4-PBE−PS hybrid and the "free" linear PS by was again found by fitting the $I(Q)-Q$ data to the form factor for a Gaussian coil[33] where this value is similar to that found by using a compact sphere Gunier analysis. As seen in the figure, the 46 kDa hybrid has a smaller R_g than a PS chain of an equal molecular weight, indicating that the hybrid is in a collapsed state. The 70 and 91 kDa hybrids have a R_g that is equal to or greater than its corresponding "free" PS chain. These results agree with those in Figure 4a; both indicate that

hybrids below a molecular weight of ∼45 kDa are more collapsed than those above ∼70 kDa, and this collapsed state transition is correlated with the dendron block transition in conformation. Further, the two solvents do not affect the transition for these systems.

To rule out the possibility of deuteration effects between the linear block and the solvent, we studied G4-PBE−PS hybrids and linear PS in THF at a concentration of 4 mg/mL via DLS to determine R_h (see Figure 4c). The 46 kDa hybrid has a smaller R_h than a corresponding PS chain, again demonstrating it is in a collapsed state. The 70 and 91 kDa hybrids have an R_h that is larger than the corresponding PS chain similar to the R_g results for the deuterated material.

It is hypothesized that the 20 kDa hybrid has the conformation of a knitted coil for the conditions studied (Figure 1). This hypothesis is supported by a dendrimer block that is a spherelike object with a radius that is about 1 nm larger that the corresponding "free" dendrimer as well as a linear block that is more contracted than its native PS chain. A more contracted linear block potentially indicates that the linear chain is weaving in and out of the dendrimer free volume, thus occupying a smaller space than if it were a free chain in solution. Comparing the size of the linear block, 3.75 ± 0.25 nm, to the size of the dendrimer block, 1.82 ± 0.01 nm, shows that some of the linear block can be shielded by the dendrimer. Our data for this system do not support an encapsulated dendrimer conformation since attempts to fit the SANS data of this system to a core−shell morphology failed.

The 45 kDa system has the linear block in a more compact form than a free dPS chain, similar to the 20 kDa system; however, the dendrimer has adopted an extended form rather than the sphere. Further, the 100 kDa hybrid has adopted a form where the linear block is essentially equivalent to an unattached linear molecule with a conelike dendrimer attached to it. It is believed that the increase in molecular weight has triggered a change from the spherical to an extended/conelike morphology, allowing the linear chain to maximize the system entropy. This is the hypothesis advanced by Jeong et al.[23] following the ideas of Skvortsov et al.[43] Basically, a chain tethered in a high-energy region (dendrimer) next to a lower energy one (free solvent) will adopt a random walk if tethered far from the interface and is of small molecular weight. However, increasing the molecular mass allows greater sampling of the lower energy region until the chain straightens within the high-energy space and adopts a random walk in the low-energy region. This appears to be similar to what we observe except the dendrimer (high-energy region) is flexible and changes shape to minimize contact with the linear macromolecule. Skvortsov et al.[43] clearly demonstrate it is the relative size of the chain to tethering distance that is key to this transition, and so it is expected that the dendrimer generation will influence the molecular weight where the morphological change occurs.

Conclusion

The conformation of linear−dendrimer diblock copolymers in solution can be probed by deuterating one block and performing a series of SANS contrast match experiments. It was found for the G4-PBE−dPS system that there is a transition from a knitted to random coil conformation upon increasing the relative molecular weight of the linear block to the dendrimer block. Further, the dendron changes shape from spherical to an extended, conelike structure. This unexpected transition is expected to be driven by the linear chain maximizing its entropy at the expense of the dendron's. We believe this shape change, if triggered through external stimuli, can be exploited in the design of a range of advanced materials ranging from sensors to molecular machines. Future research will examine these issues and the development of a viable system.

Acknowledgment. We gratefully acknowledge financial support from Michigan State University. The neutron scattering work was supported by the U.S. Department of Energy, BES-Materials Science, under Contract W-31-109-ENG-38 to the University of Chicago. We also thank Mr. Denis Wozniak and Dr. Pappannan Thiyagarajan for their assistance with the SANS experiments and discussion of results.

Supporting Information Available: Plots of I vs Q and QI vs Q for dendrimers and linear−dendrimer diblock copolymers in dilute solutions. This material is available free of charge via the Internet at http://pubs.acs.org.

References and Notes

(1) Newkome, G. R.; Moorefield, C. N.; Vögtle, F. *Dendritic Molecules: Concepts, Syntheses, Perspectives*; John Wiley & Sons: New York, 1996.
(2) Hawker, C. J.; Fréchet, J. M. J. *J. Am. Chem. Soc.* **1990**, *112*, 7638−7647.
(3) Tomalia, D.; Baker, H.; Dewald, J.; Hall, M.; Kallos, G.; Martin, S.; Roeck, J.; Ryder, J.; Smith, P. *Polym. J.* **1985**, *17*, 117−132.
(4) Chen, H.; Neerman, M. F.; Parrish, A. R.; Simanek, E. E. *J. Am. Chem. Soc.* **2004**, *126*, 10044−10048.
(5) Hahn, Uwe; Gorka, M.; Vogtle, F.; Vogtle, F.; Vicinelli, V.; Ceroni, P.; Maestri, M.; Balzani, V. *Angew. Chem., Int. Ed.* **2002**, *41*, 3595−3598.
(6) Murugan, E.,; Sherman, R. L., Jr.; Spivey, H. O.; Ford, W. T. *Langmuir* **2004**, *20*, 8307−8312.
(7) Vestberg, R.; Nilsson, C.; Lopes, C.; Lind, P.; Eliasson, B.; Malmstrom, E. *J. Polym. Sci., Part A: Polym. Chem.* **2004**, *42*, 2784.
(8) Chiba, H.; Tsururta, M.; Shiki, S.; Higuchi, M.; Yamamoto, K. *Nature (London)* **2002**, *415*, 509−511.
(9) Barbera, J.; Donnini, B.; Gimenez, R.; Guillon, D. *J. Mater. Chem.* **2001**, *11*, 2808−2813.
(10) Sashiwa, H.; Shigemasa, Y.; Roy, R. *Macromolecules* **2001**, *24*, 3211−3214.
(11) Percec, V.; Chow, W.; Ungor, G. *J. Am. Chem. Soc.* **2000**, *122*, 10273−10281.
(12) Wagner, N. J.; Tande, B. M.; Mackay, M. E.; Hawker, C. J.; Jeong, M. *Macromolecules* **2001**, *34*, 8580−8585.
(13) Chapman, T. M.; Hillyer, G. L.; Mahan, E. J.; Shaffer, K. A. *J. Am. Chem. Soc.* **1994**, *116*, 11195−11196.
(14) Cho, B. K.; Jain, A.; Gruner, S. M.; Wiesner, U. *Science* **2004**, *305*, 1598−1601.
(15) Pochan, D. J.; Pakstis, L.; Huang, E.; Hawker, C.; Vestberg, R.; Pople, J. *Macromolecules* **2002**, *35*, 9239−9242.
(16) van Hest, J. C. M.; Delnoye, D. A. P.; Baars, M. W. P. L.; van Genderen, M. H. D.; Meijer, E. W. *Science* **1995**, *268*, 1592−1595.
(17) Santini, C. M. B.; Johnson, M. A.; Boedicker, J. Q.; Hatton, T. A.; Hammond, P. T. *J. Polym. Sci., Part A: Polym. Chem.* **2004**, *42*, 2784.
(18) Aoi, K.; Motoda, A.; Okada, M.; Imae, T. *Macromol. Rapid Commun.* **1997**, *18*, 945−952.
(19) Fréchet, J. M. J.; Gitsov, I. *Macromolecules* **1993**, *26*, 6536−6546.
(20) Fréchet, J. M. J.; Dao, J.; Hawker, C. J.; Leduc, M. R. *J. Am. Chem. Soc.* **1996**, *118*, 1111−11118.
(21) Mackay, M. E.; Jeong, M.; Hony, Y.; Tande, B. M.; Wagner, N. J.; Hong, S.; Gido, S. P.; Vestberg, R.; Hawker, C. J. *Macromolecules* **2002**, *35*, 8391−8399.
(22) Gitsov, I.; Fréchet, J. M. J. *Macromolecules* **1993**, *26*, 6536−6537.
(23) Jeong, M.; Mackay, M. E.; Vestberg, R.; Hawker, C. J. *Macromolecules* **2001**, *24*, 4927−4936.
(24) Mackay, M. E. *C. R. Chim.* **2003**, *6*, 747−754.
(25) Dawking, J. V.; Pethrick, R. A. *Modern Techniques for Polymer Characterization*; John Wiley & Sons: New York, 1999.
(26) Benoit, D.; Chaplinski, V.; Braslau, R.; Hawker, C. J. *J. Am. Chem. Soc.* **1999**, *121*, 3904.
(27) DeGennes, P. G. *Scaling Properties in Polymer Physics*; Cornell University Press: Ithaca, NY, 1979.
(28) Akcasu, A. Z.; Hammouda, B. *Macromolecules* **1983**, *16*, 951−956.
(29) Takahashi, Y.; Matsumota, N.; Iio, S. Kondo, H.; Noda, I.; Imai, M.; Matsushita, Y. *Langmuir* **1999**, *15*, 4120−4122.
(30) Guinier, A.; Fournet, G. *Small Angle Scattering of X-Rays*; John Wiley & Sons: New York, 1955.

(31) Thiyagarajan, P.; Zajac, G. W.; Seifert, S.; Littrell, K. L.; Gallas, J. M. *Biophys. J.* **1999**, *77*, 1135−1142.
(32) Holtzer, A. *J. Polym. Sci.* **1955**, *17*, 432−434.
(33) Higgins, J. S.; Benoit, H. C. *Polymers and Neutron Scattering*; Clarendon Press: Oxford, 1994.
(34) Ballauff, M.; Pötschke, D.; Lindner, P.; Vögtle, F.; Fischer, M. *Macromolecules* **1999**, *32*, 4079−4087.
(35) Likos, C. N.; Ballauff, M.; Dingenouts, N.; Rosenfeldt, S.; Vögtle, F.; Werner, N.; Lindner, P. *J. Chem. Phys.* **2002**, *117*, 1869−1877.
(36) Burchard, W. *Adv. Polym. Sci.* **1999**, *143*, 113−194.
(37) Schmidt, M.; Burchard, W. *Macromolecules* **1981**, *14*, 210.
(38) Schmidt, M.; Burchard, W. *Macromolecules* **1981**, *14*, 210−211.
(39) Termeer, H. U.; Burchard, W.; Wunderlich, W. *Colloid Polym. Sci.* **1980**, *258*, 675−684.
(40) Mansfield, M. L.; Jeong, M. *Macromolecules* **2002**, *35*, 9794−9798.
(41) Mansfield, M. *Macromolecules* **2000**, *33*, 8043−8049.
(42) Hjelm, R. P. *J. Appl. Crystallogr.* **1985**, *18*, 452−460.
(43) Skvortsov, A. M.; Klushin, L. I.; vanMale, J.; Leermakers, F. A. M. *J. Chem. Phys.* **2001**, *115*, 1586−1595.

MA0517291